α-Synuclein Controls Mitochondrial Calcium Homeostasis by Enhancing Endoplasmic Reticulum-Mitochondria Interactions*

Tito Calì[‡1], Denis Ottolini[§1], Alessandro Negro[§], and Marisa Brini[‡2]

From the ‡Department of Comparative Biomedicine and Food Science and the §Department of Biomedical Sciences, University of Padova, Padova 35131, Italy

Background: α-Synuclein has a central role in Parkinson disease, and it has been proposed to regulate mitochondrial morphology and autophagic clearance.
Results: α-Synuclein overexpression augments mitochondrial Ca^{2+} transients by enhancing endoplasmic reticulum-mitochondria interactions.
Conclusion: Physiological levels of α-synuclein are required to sustain mitochondrial function and morphology integrity.
Significance: Mitochondrial Ca^{2+} represents an important site where α-synuclein can modulate cell bioenergetics and survival.

α-Synuclein has a central role in Parkinson disease, but its physiological function and the mechanism leading to neuronal degeneration remain unknown. Because recent studies have highlighted a role for α-synuclein in regulating mitochondrial morphology and autophagic clearance, we investigated the effect of α-synuclein in HeLa cells on mitochondrial signaling properties focusing on Ca^{2+} homeostasis, which controls essential bioenergetic functions. By using organelle-targeted Ca^{2+}-sensitive aequorin probes, we demonstrated that α-synuclein positively affects Ca^{2+} transfer from the endoplasmic reticulum to the mitochondria, augmenting the mitochondrial Ca^{2+} transients elicited by agonists that induce endoplasmic reticulum Ca^{2+} release. This effect is not dependent on the intrinsic Ca^{2+} uptake capacity of mitochondria, as measured in permeabilized cells, but correlates with an increase in the number of endoplasmic reticulum-mitochondria interactions. This action specifically requires the presence of the C-terminal α-synuclein domain. Conversely, α-synuclein siRNA silencing markedly reduces mitochondrial Ca^{2+} uptake, causing profound alterations in organelle morphology. The enhanced accumulation of α-synuclein into the cells causes the redistribution of α-synuclein to localized foci and, similarly to the silencing of α-synuclein, reduces the ability of mitochondria to accumulate Ca^{2+}. The absence of efficient Ca^{2+} transfer from endoplasmic reticulum to mitochondria results in augmented autophagy that, in the long range, could compromise cellular bioenergetics. Overall, these findings demonstrate a key role for α-synuclein in the regulation of mitochondrial homeostasis in physiological conditions. Elevated α-synuclein expression and/or eventually alteration of the aggregation properties cause the redistribution of the protein within the cell and the loss of modulation on mitochondrial function.

Parkinson disease (PD)[3] is a common neurodegenerative disease characterized by the loss of dopaminergic neurons in the substantia nigra pars compacta (1) and formation of intraneuronal protein aggregates called Lewy bodies (2). The etiology of the disease is still unknown but probably involves a combination of genetic and environmental factors inducing mitochondrial dysfunctions (3).

Specific mutations in nuclear genes encoding α-synuclein (α-syn), DJ-1, LRRK2, PINK1, and parkin as well as within the mtDNA were identified in familial forms of PD (about 5–10% of cases), giving the possibility, by manipulating their expression levels in cellular and animal models, to investigate their physiological function and early pathogenic changes that may lead to neurodegeneration.

α-syn, a major component of Lewy bodies, is a small protein of 140 amino acids prevalently localized in the cytosolic compartment at the presynaptic level in neurons. Recently, it was also shown to localize to mitochondria (4, 5) and to contain a mitochondrial targeting sequence (6). α-syn function is still unclear, but emerging evidence suggests that it interacts with phospholipids membranes acting as critical regulator of vesicle dynamics at the synapse (7–9). Despite that the interpretation of the various phenotypes caused by wt or mutant α-syn overexpression and/or α-syn deficiency is complex and remains sometime controversial, alterations of mitochondrial function have been clearly documented in different cellular and animal models by several groups. α-syn accumulation has been associated with mitochondrial complex I dysfunction (6, 10, 11), and α-syn null mice display striking resistance to the neurotoxin 1-methyl-4-phenyl-1,2,3,6-tetrahydropyridine (MPTP)-induced degeneration of dopaminergic neurons and dopamine release (12,

---

[1] Both are joint first authors.
[2] To whom correspondence should be addressed: Dept. of Comparative Biomedicine and Food Science, University of Padova, Viale G. Colombo, 3, 35131 Padova, Italy. Tel.: 39-049-8276150; Fax: 39-049-8276125; E-mail: marisa.brini@unipd.it.

[3] The abbreviations used are: PD, Parkinson disease; α-syn, α-synuclein; mtRFP, mitochondria-targeted RFP; mtGFP, mitochondria-targeted GFP; ER, endoplasmic reticulum; erGFP, ER-targeted GFP; TMRM, tetramethylrhodamine methyl ester; VPA, valproic acid; TAT, Trans-Activator of Transcription; mtAEQ, mitochondrial aequorin; cytAEQ, cytosolic wt aequorin; erAEQ, ER-targeted aequorin; KRB, Krebs-Ringer modified buffer; IB, intracellular buffer; FCCP, carbonyl cyanide p-trifluoromethoxyphenylhydrazone; InsP$_3$, inositol 1,4,5 trisphosphate.

13). Mitochondrial defects including altered morphology, loss of mitochondrial membrane potential, increased mitochondrial ROS, reduced complex I activity, and cytochrome c release were observed in $α$-syn transgenic mice (14) and in cells overexpressing $α$-syn (4, 15, 16). Recently, it has been shown that $α$-syn directly regulated the mitochondria dynamics by participating in the fusion/fission process and autophagy (17–19).

The molecular mechanisms underlying the observed dysfunctions need to be elucidated, and we decided to investigate the role of $α$-syn in mitochondrial function by overexpressing it in an exogenous system, SH-SY5Y or HeLa cells, and analyzing the effects on Ca^{2+} homeostasis in living cells. By directly measuring mitochondrial Ca^{2+} dynamics and by monitoring mitochondria morphology in living cells, we have found that $α$-syn is essential to control mitochondrial Ca^{2+} homeostasis and mitochondrial architecture, playing a role in modulating the contacts between mitochondria and endoplasmic reticulum (ER). In addition, we have found that the observed effects are dependent both to $α$-syn cytosolic distribution and abundance, as its redistribution to localized foci or its silencing abolished enhanced mitochondrial Ca^{2+} uptake. Thus $α$-syn is essential to sustain mitochondrial functions; when this action is lost the autophagic response is augmented.

This $α$-syn function certainly adds further complexity to the multifaceted nature of PD-related proteins, but the findings are particularly interesting, underlining the possibility that the modulation of ER-mitochondria cross-talk may represent a common pathway in neurodegeneration.

EXPERIMENTAL PROCEDURES

DNA Constructs—Plasmids encoding wt and $α$-syn-(1–97) and TAT-fusion wt $α$-syn recombinant proteins were previously described (20). C-terminal Myc-tagged $α$-syn-(1–97) construct was generated by PCR amplification using the forward (5′-GAAGTTCGAATTCATGGATGTATTCATGA-AAGGACT-3′) and reverse (5′-ACTTCTCACTCGAGTTA-CAGATCTTCTTCAGAAATAAGTTTTTGTTCCTTTTT-GACAAAGCCAGTGGCTGC-3′) and cloned in pcDNA3 expression vector. The construct was verified by sequencing. Mitochondria-targeted RFP and GFP (mtRFP and mtGFP) and ER-targeted GFP (erGFP) expression vectors were kindly provided by Prof. R. Rizzuto, University of Padova. Plasmids encoding recombinant targeted aequorin probes were previously described (21).

Cell Cultures and Transfection—HeLa cells and SH-SY5Y neuroblastoma cells were grown in Dulbecco's modified Eagle's medium high glucose (DMEM, Euroclone) supplemented with 10% fetal bovine serum (FBS, Euroclone), 100 units/ml penicillin, and 100 $μ$g/ml streptomycin; 12 h before transfection, cells were seeded onto 13-mm (for aequorin measurements) or 24-mm (for tetramethylrhodamine methyl ester (TMRM) and ER-mitochondria contact sites analysis) glass coverslips and allowed to grow to 60–80% confluence. For Ca^{2+} and TMRM measurements, HeLa cells were co-transfected with aequorin and GFP/RFP constructs, respectively, and empty vector (mock) or $α$-syn expressing plasmids in a 1:2 ratio with the calcium-phosphate procedure as previously described (22). SH-SY5Y neuroblastoma cells were transfected by using the

TransFectin Lipid Reagent (Bio-Rad) according to the manufacturer's instructions. Ca^{2+} measurements were performed 36 h later. Cells plated for Western blotting were collected 24–36 h after transfection. For TAT-mediated delivery, recombinant TAT fusion proteins were added directly onto the seeded aequorin-transfected cells and incubated for 2.5–5 h in DMEM, 10% FBS, and antibiotics at 37 °C in a 5% CO_2 atmosphere. After incubation with TAT fusion proteins, the cells were extensively washed with PBS before starting Ca^{2+} measurements. In the case of valproic acid (VPA) incubation, the cells were treated for 6 days in DMEM, 10% FBS, and antibiotics at 37 °C in 5% CO_2 atmosphere and the day before the experiment transfected with mtAEQ or mtRFP. Where indicated the cells were treated with bafilomycin A1 (Sigma) 100 $μ$M for 16 h.

Antibodies—Mouse monoclonal anti-$α$-syn antibody (sc-12767, Santa Cruz Biotechnology, Inc.) was used at a 1:30 dilution in immunocytochemistry analysis and at a 1:500 dilution in Western blotting analysis. Mouse monoclonal anti-$β$-actin (AC-15, Sigma) was used at a 1:90,000 dilution in Western blotting. Mouse anti-Myc (4A6, Millipore) was used at a 1:50 dilution in immunocytochemistry and 1:2000 in Western blotting analysis. Rabbit polyclonal anti-LC3 antibody (LC3B, #2775 Cell Signaling) and rabbit polyclonal anti-p62 antibody (p62, #p0067 Sigma) were used at 1:750 and 1:1000 dilutions, respectively, in Western blotting analysis.

Immunocytochemistry Analysis—Transfected HeLa cells plated on coverslips were fixed with 3.7% formaldehyde in phosphate-buffered saline (PBS; 140 mM NaCl, 2 mM KCl, 1.5 mM KH_2PO_4, 8 mM Na_2HPO_4, pH 7.4) for 20 min and washed 3 times with PBS. Cell permeabilization was performed by 20 min of incubation in 0.1% Triton X-100 PBS followed by 30 min wash in 1% gelatin (type IV, from bovine skin, Sigma) in PBS at room temperature. The coverslips were then incubated for 90 min at 37 °C in a wet chamber with the specific antibody diluted in PBS. Staining was revealed by the incubation with specific AlexaFluor 488 or 594 secondary antibodies for 45 min at room temperature (1:100 dilution in PBS; Invitrogen). Fluorescence was analyzed with a Zeiss Axiovert microscope equipped with a 12-bit digital cooled camera (Micromax-1300Y; Princeton Instruments Inc., Trenton, NJ) or Leica Confocal SP2 microscope. Images were acquired by using Axiovision 3.1 or Leica AS software. Where indicated, raw images were smoothed by applying the Gaussian blur filter of the Image J 1.45e software for mitochondrial network morphology assessment.

Aequorin Measurements—Mitochondrial low affinity aequorin (mtAEQ) and cytosolic wt aequorin (cytAEQ) were reconstituted by incubating cells for 3 h (cytAEQ) or 1.5 h (mtAEQ) with 5 $μ$M wt coelenterazine (Invitrogen) in DMEM supplemented with 1% fetal bovine serum at 37 °C in a 5% CO_2 atmosphere. To functionally reconstitute low affinity ER-targeted aequorin (erAEQ), the ER Ca^{2+} content had to be drastically reduced. To this end, cells were incubated for 1.5 h at 4 °C in Krebs-Ringer modified buffer (KRB,125 mM NaCl, 5 mM KCl, 1 mM Na_3PO_4, 1 mM $MgSO_4$, 5.5 mM glucose, 20 mM HEPES, pH 7.4, 37 °C) supplemented with the Ca^{2+} ionophore ionomycin (5 $μ$M), 600 $μ$M EGTA, and 5 $μ$M coelenterazine (Invitrogen). Cells were then extensively washed with KRB supplemented with 2% bovine serum albumin and 1 mM EGTA (21).

After reconstitution, cells were transferred to the chamber of a purpose-built luminometer, and Ca^{2+} measurements were started in KRB medium added with 1 mM $CaCl_2$ or 100 μM EGTA or 1 mM EGTA according the different protocols and aequorin probes. 100 μM histamine in HeLa cells or 100 nM bradykinin were added as specified in the figure legends.

For mitochondrial Ca^{2+} measurements in permeabilized cells after reconstitution, the cells were transferred in an intracellular buffer (IB) (130 mM KCl, 10 mM NaCl, 0.5 mM KH_2PO_4, 1 mM $MgSO_4$, 5 mM sodium succinate, 3 mM $MgCl_2$, 20 mM HEPES, 5.5 mM glucose, 1 mM pyruvic acid supplemented with 2 mM EGTA, and 2 mM HEDTA, pH 7.0) and then permeabilized in the same buffer supplemented with 25 μM digitonin for 1 min. Cells were then perfused with IB/EGTA containing 1 mM ATP (IB/EGTA-ATP) and transferred to the luminometer chamber. Ca^{2+} uptake into mitochondria was initiated by replacing IB/EGTA-ATP buffer with IB containing a 2 mM EGTA-HEDTA-buffered Ca^{2+} of 1 μM, prepared as elsewhere described (23, 24).

All the experiments were terminated by cell lysis with 100 μM digitonin in a hypotonic Ca^{2+}-rich solution (10 mM $CaCl_2$ in H_2O) to discharge the remaining reconstituted active aequorin pool. The light signal was collected and calibrated off-line into Ca^{2+} concentration values using a computer algorithm based on the Ca^{2+} response curve of wt and mutant aequorin as previously described (25, 26).

Western Blotting Analysis—HeLa cells were flooded on ice with 20 mM ice-cold *N*-ethylmaleimide in PBS to prevent postlysis oxidation of free cysteines. Cell extracts were prepared by solubilizing cells in ice-cold 2% CHAPS in Hepes-buffered saline (50 mM HEPES, 0.2 M NaCl, pH 6.8) containing *N*-ethylmaleimide, 1 mM PMSF, and mixture protease inhibitors (Sigma). Postnuclear supernatants were collected after 10 min of centrifugation at 10,000 × *g* at 4 °C. The total protein content was determined by the Bradford assay (Bio-Rad). Samples were loaded on a 15% SDS-PAGE Tris/HCl gel, transferred onto PVDF membranes (Bio-Rad), and incubated overnight with the specific primary antibody at 4 °C. Detection was carried out by incubation with secondary horseradish peroxidase-conjugated anti-rabbit or anti-mouse IgG antibody (Santa Cruz Biotechnology) for 1.5 h at room temperature. The proteins were visualized by the chemiluminescent reagent Immobilon Western (Millipore). Densitometric analyses were performed by using Kodak1D image analysis software (Kodak Scientific Imaging Systems, New Haven, CT). Means of densitometric measurements of at least three independent experiments, normalized by the endogenous *β*-actin values, were compared by Student's *t* test.

siRNA-mediated Knockdown—HeLa cells were transfected with cell validated predesigned siRNA oligonucleotides (Qiagen) directed against human *α*-syn (Hs_SNCA_5 siRNA, SI03026478, Target transcript: NM_000345) using the Attractene reagent (Qiagen), which is also highly suitable for cotransfection of plasmid DNA with siRNA. The siRNA transfection protocol was adjusted according to the manufacturer's instructions (18 pmol of each siRNA oligo were added for each 2 μl of Attractene). RNAi negative control duplex, *i.e.* scramble siRNA (which sequence matched no known mRNA sequence in the vertebrate genome) was purchased from Qiagen (AllStars Neg. siRNA AF 488, 1027284). Briefly, the day before the experiment the cells were seeded at 70–80% confluence in a 24-well plate in 500 μl of culture medium containing serum and antibiotics. The day after, transfection complexes were added dropwise and incubated under normal growth conditions. Gene down-regulation and mitochondrial Ca^{2+} transients were monitored after 36–48 h after transfection.

TMRM Analysis—The TMRM "non-quenching" method was used, which is adequate for the comparison of the membrane potential between two populations of cells (27), and thus a decrease in TMRM signal reflected mitochondrial depolarization. HeLa cells seeded on coverslips were cotransfected with *α*-syn-expressing plasmid and cytosolic-GFP as a marker of cotransfection, and 30 h after transfection cells were loaded with 20 nM TMRM for 30 min at 37 °C in KRB containing 1 mM $CaCl_2$ and 5.5 mM glucose. TMRM fluorescence was registered at a 510-nm wavelength with a Leica SP2 confocal microscope at 40× magnification. The normalized TMRM fluorescence intensity was obtained by acquiring images before and after application of 10 μM proton ionophore carbonyl cyanide *p*-trifluoromethoxyphenylhydrazone (FCCP) to redistribute TMRM away from mitochondria. Measurements were corrected for residual TMRM fluorescence after full $\Delta\psi_m$ collapse with FCCP. Basal average TMRM signal was normalized to the average remaining signal obtained upon FCCP treatment and shown as Δ fluorescence above the threshold. Regions of interest were off-line-positioned across the peripheral cell area, and TMRM fluorescence was analyzed using ImageJ software.

Analysis of Mitochondrial Morphology—mtRFP fluorescence from positive-cotransfected cells was used to reveal mitochondrial morphology.

Cells that displayed a network of filamentous mitochondria were classified as normal (not fragmented), and cells with fragmented or partially truncated mitochondria were classified as fragmented (see representative images in Fig. 3*C*). To evaluate mitochondrial shape, fluorescence microscopy images of randomly selected fields were acquired, and every single mitochondrion of the investigated cells was marked to analyze morphological characteristics such as its area, perimeter, and major and minor axes. On the basis of these parameters, the mitochondrion circularity and its form factor ($4\pi \times$ area/perimeter^2 (28)), consistent with a measure of mitochondrial length and the degree of branching, were calculated as described in Dagda *et al.* (29).

ER-mitochondria Contact Site Analysis—Cells plated on 24-mm-diameter coverslips were transfected with erGFP and mtRFP together with empty or *α*-syn or *α*-syn-(1–97)-expressing vectors. Fluorescence was analyzed in living cells by a Leica SP2 confocal microscope. Cells were excited separately at 488 or 543 nm, and the single images were recorded. Confocal stacks were acquired every 0.2 μm along the *z* axis (for a total of 40 images) with a 63× objective. Cells were maintained in KRB containing 1 mM $CaCl_2$ and 5.5 mM glucose during acquisition of images. For mitochondria-ER interaction analysis, stacks were automatically thresholded using ImageJ, deconvoluted, three-dimensional-reconstructed, and surface-rendered by using VolumeJ (ImageJ). Interactions were quantified by

Manders' colocalization coefficient as already described (30, 31).

Statistical Analysis—Data are reported as the means ± S.E. Statistical differences were evaluated by Student's two-tailed *t* test for impaired samples, with *p* value 0.01 considered statistically significant.

RESULTS

Subcellular Localization of Overexpressed α-Synuclein and Effects on Calcium Homeostasis—The effects of α-syn overexpression were investigated by overexpressing it in dopaminergic neurons, the human neuroblastoma cells line SH-SY5Y, and in HeLa cells and analyzing the impact on Ca^{2+} signaling. Analysis of intracellular Ca^{2+} homeostasis was performed using aequorin probes targeted to the mitochondrial matrix (mtAEQ), to the cytosol (cytAEQ), or to the lumen of the ER (erAEQ) (21). The expression level and subcellular localization of overexpressed wt α-syn were first verified. Western blotting analysis was performed on transfected SH-SY5Y or HeLa cells and showed a significant increase in α-syn expression compared with the endogenous level of empty vector-transfected cells (Fig. 1*A*). The endogenous level of α-syn in SH-SY5Y cells was hardly detectable. Equal loading of proteins was verified by probing the membrane with an anti-β-actin antibody, and quantification by densitometric analysis on the whole population revealed an increase of about 50% (100 ± 9.64% in mock cells *versus* 147.69 ± 9.87% in α-syn-overexpressing HeLa cells, *p* < 0.01, *n* = 3). However, considering that the average of transient transfections in HeLa cells was about of 25%, the overexpression of α-syn in transfected cells approached about 3-fold with respect to the endogenous content. Immunofluorescence experiments performed in HeLa and in SH-SY5Y neuroblastoma cells revealed a diffuse cytosolic staining with no nuclear exclusion (Fig. 1*B*). Negative untransfected cells showing the endogenous levels of α-syn are visible in the panel relative to HeLa cells. SH-SY5Y untransfected cells show no fluorescence signal. The possible co-localization of α-syn and mitochondria was investigated by co-expressing α-syn and mtRFP probe in HeLa cells; no clear signal in mitochondria was detected with anti-α-syn antibodies, and the merging picture failed to reveal co-localization, indicating that the overexpressed α-syn was prevalently cytosolic (Fig. 1*C*). Furthermore, mtRFP failed to reveal morphological alterations in mitochondria of α-syn-overexpressing cells, as it showed the typical filamentous structure of mitochondrial network (see the *Gaussian blur panel*) as well as in cells transfected only with mtRFP (*right panel* of Fig. 1*C*).

Then measurements of mitochondrial Ca^{2+} transients generated by cell stimulation were carried out using mtAEQ (21). Representative traces of typical experiments and statistical analysis are shown in Fig. 1, *D* and *E*. Where indicated, cells were exposed to 100 nM bradykinin (BK) or 100 μM histamine (His), causing the generation of inositol 1,4,5 trisphosphate ($InsP_3$) and the consequent opening of the $InsP_3$ channels of the intracellular stores. Fig. 1*D* refers to SH-SY5Y, and Fig. 1*E* refers to HeLa cells; mitochondrial Ca^{2+} transients in α-syn-overexpressing cells were significantly higher than those observed in control cells (peak values: 53.5 ± 2.76 μM in control

SH-SY5Y cells, *n* = 11, *versus* 70.6 ± 2.88 μM in α-syn-overexpressing SH-SY5Y cells, *n* = 14, *p* < 0.0005 and 116.52 ± 2.84 μM in control HeLa cells, *n* = 10, *versus* 140.74 ± 5.7 μM in α-syn-overexpressing HeLa cells, *n* = 9, *p* < 0.001), indicating that the observed effects were not cell type-specific. To verify whether α-syn could play a general role in Ca^{2+} homeostasis, Ca^{2+} measurements were also performed in the cytosol and in the lumen of the ER by using specifically targeted aequorin probes. Fig. 1, *F* and *G*, showed no significant differences between α-syn-overexpressing and control HeLa cells (cytosolic peak values: 3.33 ± 0.04 μM in control cells, *n* = 14, *versus* 3.24 ± 0.04 μM in α-syn-overexpressing cells, *n* = 13; ER Ca^{2+} levels: 424.00 ± 18.40 μM in control cells, *n* = 15, *versus* 415.90 ± 24.00 μM in α-syn-overexpressing cells, *n* = 13), highlighting the possibility that α-syn may have a specific mitochondrial role.

Cytosolic and ER Ca^{2+} measurements in SH-SY5Y cells also failed to reveal differences between controls and α-syn-overexpressing cells (not shown). To avoid possible biochemical alterations associated with increased α-syn levels and dopamine oxidation in dopaminergic SH-SY5Y cells, it was decided to perform the following experiments only in HeLa cells.

Mitochondrial Ca^{2+} Uptake Machinery Was Not Modified by α-Synuclein Overexpression—Mitochondrial Ca^{2+} accumulation depends on the proton electrochemical gradient that drives rapid accumulation of cations across the ion-impermeant mitochondrial inner membrane and on the mitochondrial Ca^{2+} uniporter that, upon cell stimulation, is exposed to microdomains of high Ca^{2+} concentration that well match its low Ca^{2+} affinity and are sensed thanks to the close contact of mitochondria with ER Ca^{2+} channels (32). To investigate whether the overexpressed α-syn could directly interfere with the mitochondrial Ca^{2+} transport machinery, mitochondrial Ca^{2+} uptake in α-syn-overexpressing cells was investigated in permeabilized cells exposed to fixed Ca^{2+} concentration solution. Briefly, transfected HeLa cells were perfused with a solution mimicking the intracellular milieu (IB), supplemented with 2 mM EGTA, and permeabilized with 25 μM digitonin for 1 min (for details see "Experimental Procedures"). Then the perfusion buffer was changed to IB/EGTA-ATP-buffered Ca^{2+} of 1 μM, eliciting a gradual rise in mitochondrial Ca^{2+} concentration ($[Ca^{2+}]_m$) that reached a plateau value of ~30 μM (31.43 ± 1.27 μM in mock cells, *n* = 16, *versus* 30.86 ± 2.07 μM in α-syn-overexpressing cells, *n* = 14) (Fig. 2*A*). In α-syn-overexpressing HeLa cells, the $[Ca^{2+}]_m$ increase was similar to that observed in controls. To exclude that the absence of effects was due to the release of α-syn after digitonin treatment, immunocytochemistry analysis was performed on permeabilized cells, and Fig. 2*B* showed diffuse intracellular α-syn distribution as in control cells. Because α-syn is not released after cell permeabilization, it is plausible to think that, due to its propensity to interact with lipids and membrane (33), it could be associated directly (or indirectly through other proteins) to intracellular membranes, including mitochondrial membranes as previously shown (34). Then mitochondrial membrane potential ($\Delta\psi_m$) was estimated in resting conditions by loading cells with the potential-sensitive probe TMRM. The results shown in Fig. 2*C* revealed no significant differences in the TMRM fluorescence measured in
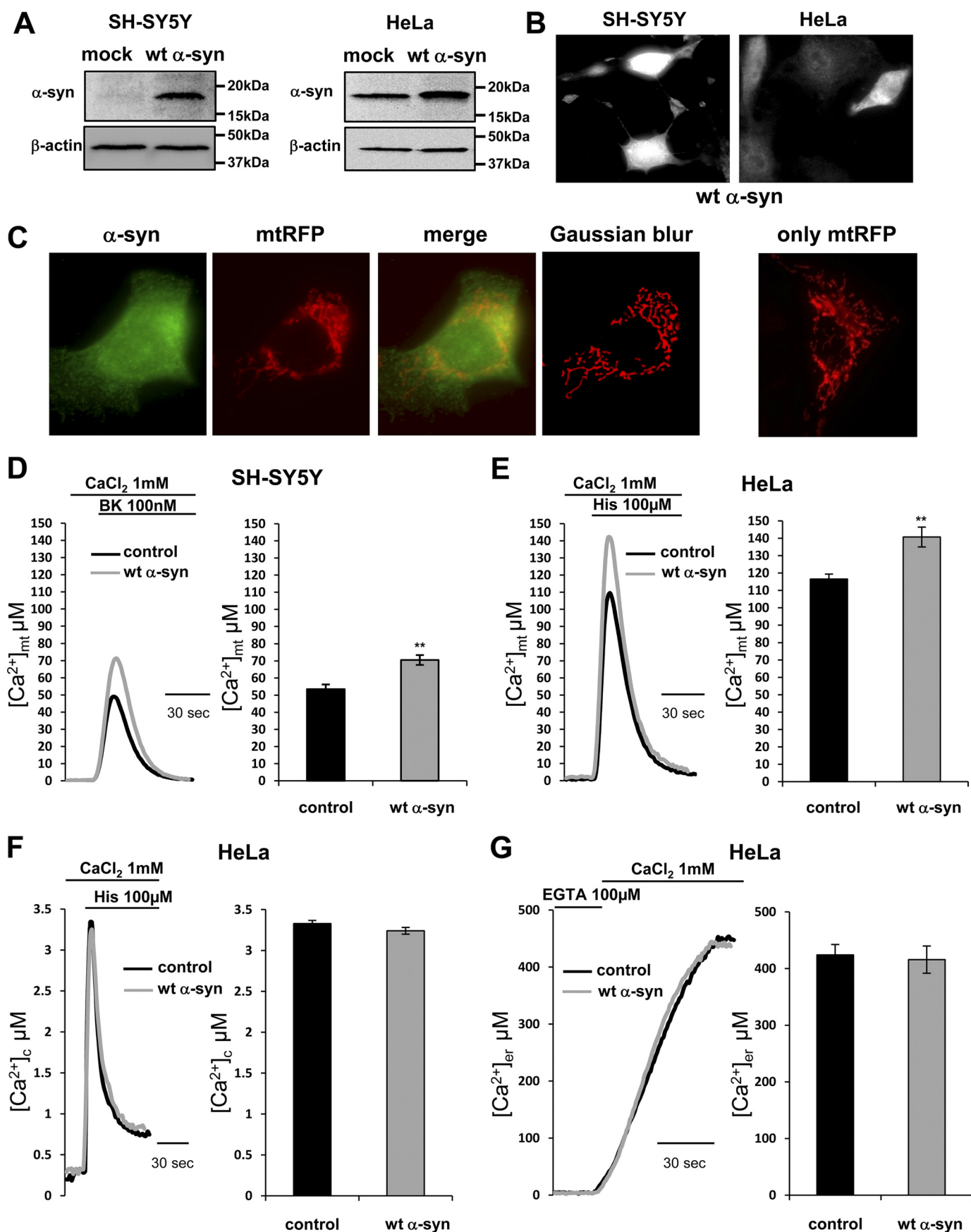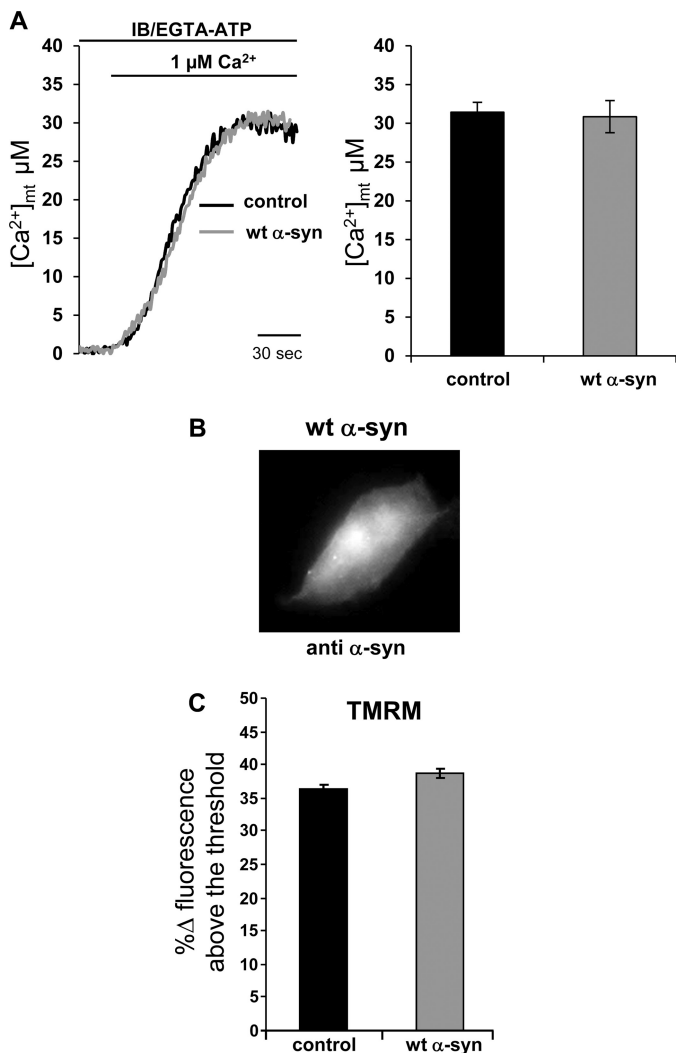
FIGURE 2. Mitochondrial Ca²⁺ uptake in permeabilized cells and mitochondrial membrane potential are not affected by wt α-synuclein over-expression. *A*, shown are representative traces (*left*) and average plateau $[Ca^{2+}]_m$ values (*right*, results are the mean $\pm$ S.E.) reached in permeabilized cells exposed to 1 μM Ca²⁺-buffered solution. Where indicated, the medium was switched from IB/EGTA-ATP to IB/1 μM Ca²⁺. The traces are representative of at least 14 independent experiments. *B*, shown is immunocytochemistry analysis on permeabilized HeLa cells overexpressing wt α-syn. The staining with monoclonal antibody against α-syn was revealed by AlexaFluor 488-conjugated antibody. *C*, HeLa cells (control and overexpressing wt α-syn) were loaded with TMRM probe to determine the mitochondrial membrane potential ($\Delta\Psi$). *Bars* represent the average TMRM fluorescence signals subtracted of signals remaining after FCCP treatment to collapse $\Delta\Psi$ and are expressed as % Δ fluorescence. The analysis was performed on $n = 124$ mock cells and on $n = 209$ α-syn-overexpressing cells.

α-syn-overexpressing cells compared with the control ($36.16 \pm 0.99\%$ in mock cells, $n = 124$, cells *versus* $38.81 \pm 0.67\%$ in α-syn-overexpressing cells, $n = 209$ cells), indicating that the

driving force for mitochondrial Ca²⁺ accumulation is equivalent in the two cell batches.

Threshold Levels of Endogenous α-Synuclein Are Required to Maintain Mitochondrial Network Architecture and Ca²⁺ Homeostasis—To address the possible role of α-syn in mitochondrial Ca²⁺ homeostasis, a siRNA-mediated silencing of endogenous α-syn was performed in HeLa cells, and mitochondrial Ca²⁺ measurements were carried out in these cells. Efficient knockdown of endogenous α-syn has been determined by Western blotting analysis. As shown in Fig. 3*A*, treatment with a siRNA specific for α-syn led to a ≈ 70% reduction of the endogenous protein level compared with cells treated with a scrambled control siRNA. The quantification was carried out by densitometric analysis, and the α-syn levels were normalized with respect to the β-actin levels as indicated in the histograms.

Mitochondrial Ca²⁺ measurements were performed after α-syn-mediated siRNA knockdown. As shown in Fig. 3*B*, down-regulation of the α-syn intracellular level is associated with a concomitant reduction in the mitochondria ability to take up Ca²⁺, the mitochondrial peak height being of 108.75 ± 3.60 μM in scrambled siRNA control cells, $n = 8$, *versus* 74.28 ± 2.53 μM in α-syn siRNA-treated cells, $n = 10$, $p < 0.0001$. To investigate the morphology of mitochondria, α-syn siRNA-treated HeLa cells were co-transfected with mtRFP and observed under a fluorescent microscope (Fig. 3*C*). When the scramble siRNA was applied, the majority of mtRFP-positive cells showed an intact network of tubular mitochondria, but interestingly, upon down-regulation of α-syn expression, the percentage of cells with truncated or fragmented mitochondria was significantly increased from about 15% in scramble siRNA-treated cells up to 70% in α-syn siRNA-treated cells. The analysis was performed on $n = 33$ cells from 2 independently transfected coverslips of each batch. Mitochondria morphology was classified as "tubular" or "fragmented" according to the images shown in Fig. 3*C*. Mitochondrial morphology was also quantified in the two batches of mtRFP-positive cells using ImageJ software (Fig. 3*D*). Evaluation of mitochondria circularity (as index of elongation) and form factor (as index of elongation and degree of branching) revealed a reduction both in elongation and in branching in α-syn siRNA-treated cells with respect to scrambled siRNA control cells (the value of 1 corresponding to a perfect circle (35)).

To establish a relationship between α-syn levels and mitochondrial Ca²⁺ signaling, we decided to modify its endogenous content by treating HeLa cells with VPA. VPA has been shown to cause a robust dose- and time-dependent increase in the levels of endogenous α-syn protein and mRNA (36). A 6-day treatment of HeLa cells with VPA caused a dose-dependent

FIGURE 1. Western blotting analysis, immunolocalization, and Ca²⁺ measurements in wt α-synuclein-overexpressing cells. SH-SY5Y or HeLa cells were transfected with wt α-syn expression plasmid and analyzed by Western blotting (*A*) or immunocytochemistry (*B*). *C*, shown are HeLa cells co-transfected with mtRFP and α-syn or transfected with mtRFP only. The merge image revealed no colocalization between α-syn and mtRFP. Gaussian blur analysis was performed with ImageJ software to remove the signal out of focus. mtRFP fluorescence revealed intact filamentous mitochondrial morphology in α-syn-expressing cells as in cells transfected only with mtRFP. Mitochondrial Ca²⁺ transients, $[Ca^{2+}]_m$, in SH-SY5Y (*D*) or HeLa cells (*E*) overexpressing α-syn are shown. Cells were transfected with mtAEQ (control) or co-transfected with mtAEQ and wt α-syn. *Bars* represent the mean $[Ca^{2+}]$ values upon stimulation. Results are the mean $\pm$ S.E. **, $p < 0.001$. The traces are representative of at least nine independent experiments. Cytosolic ($[Ca^{2+}]_c$) (*F*) and ER ($[Ca^{2+}]_{er}$) (*G*) Ca²⁺ concentration in HeLa cells overexpressing wt α-syn are shown. Cells were transfected with cytAEQ or erAEQ (control) or co-transfected with cytAEQ or erAEQ and wt α-syn. *Bars* represent the mean $[Ca^{2+}]$ values upon stimulation (*F*) and resting $[Ca^{2+}]$ (*G*). Results are the mean $\pm$ S.E. *Panel G* shows the kinetics of ER refilling upon re-addition of CaCl₂ 1 mM to Ca²⁺-depleted cells (see "Experimental Procedures"). The traces are representative of at least 13 independent experiments. Where indicated 100 nM bradykinin or 100 μM histamine, two InsP₃ generating agonists, were applied.
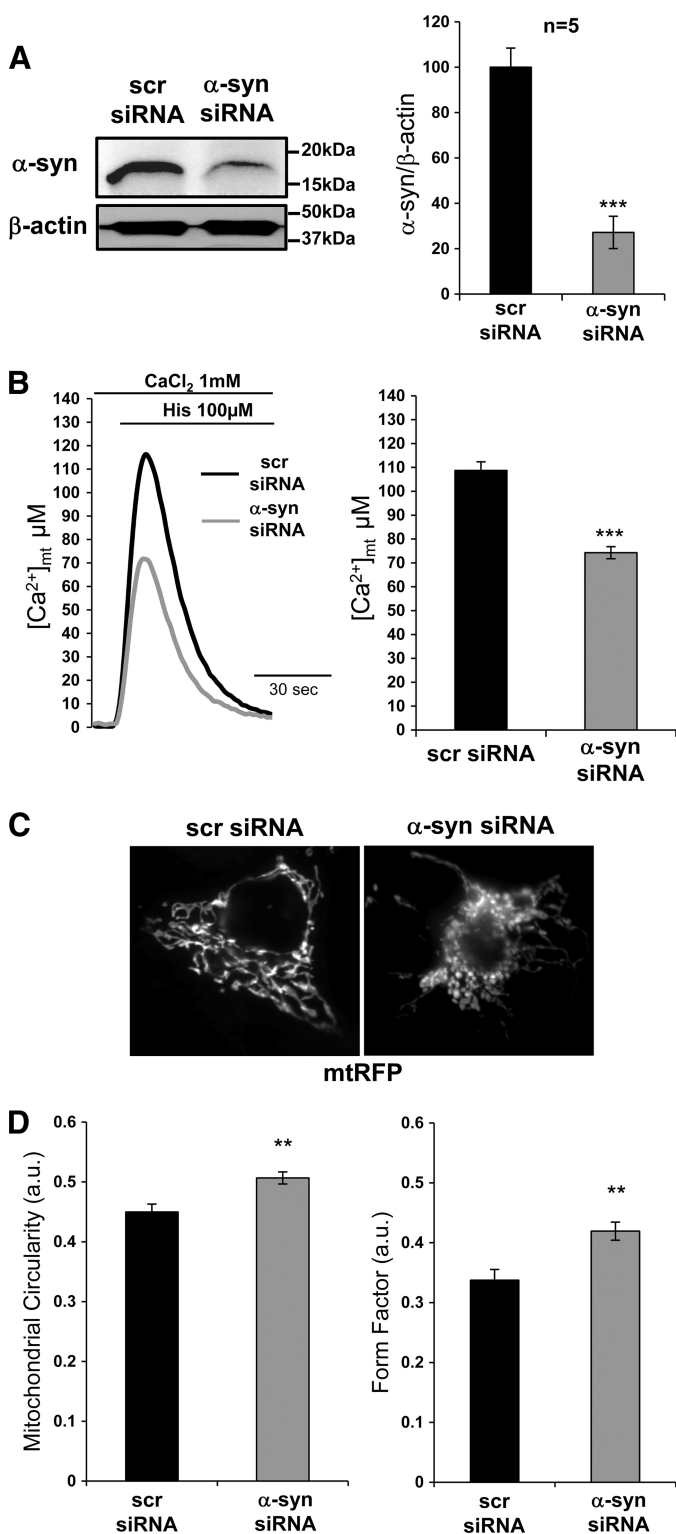
FIGURE 3. Silencing of α-synuclein impairs mitochondrial Ca²⁺ transients and morphology. *A,* shown are Western blotting and densitometric analysis of siRNA-mediated silencing of endogenous α-syn in HeLa cells. Results are the mean ± S.E. ***, $p < 0.0001$. *B,* mitochondrial Ca²⁺ transients were induced by cell stimulation, where 100 μM histamine was applied. The traces are representative of at least eight independent experiments. *Bars* indicate the average heights of peak values. Results are the mean ± S.E. ***, $p < 0.0001$. *C,* α-syn siRNA or Scr siRNA and mtRFP were co-transfected in HeLa cells. After 36–48 h cells were observed under fluorescence microscope to evaluate mitochondrial morphology. The panel displays representative mitochondrial phenotypes observed

increase in α-syn protein levels, as documented by Western blotting analysis and quantification by densitometric analysis (Fig. 4*A*). Immunocytochemistry analysis also revealed a marked increase of the α-syn signal upon VPA treatment and more strikingly highlighted a dose-dependent intracellular redistribution of α-syn (Fig. 4*B*). Indeed, in cells exposed to high doses of VPA (≥250 μM), the antibody against α-syn revealed the formation of cytoplasmic foci reminiscent of stalled vesicles, as previously described (7, 37). Mitochondrial Ca²⁺ measurements in cells treated with increasing doses of VPA (from 0.1 μM up to 1 mM) revealed a significant increase in mitochondrial Ca²⁺ uptake capacity at low VPA doses followed by a dose-dependent significant decrease at high doses (≥250 μM). Fig. 4, *C* and *D*, show the statistical analysis and representative experiments, with average Ca²⁺ peak values of 113.71 ± 3.57 μM in control cells (mtAEQ) $n = 16$, 143.95 ± 2.69 μM in α-syn-overexpressing cells $n = 16$ $p < 0.0001$, 133.91 ± 2.50 μM $n = 6$ $p < 0.005$ in 0.1 μM VPA treated cells, 115.22 ± 4.59 μM $n = 5$ in 10 μM VPA-treated cells, 94.63 ± 3.32 μM $n = 6$ in 250 μM VPA-treated cells $p < 0.01$, and 83.16 ± 1.86 μM $n = 6$ in 1 mM VPA-treated cells $p < 0.001$. To exclude the possibility that high doses of VPA could be toxic and thus damage the mitochondria, thus explaining the observed phenotype, the mitochondrial network integrity upon VPA treatment was explored by monitoring fluorescence in mitochondria labeled with mtRFP or mtGFP. Fig. 4*E* shows that VPA treatment does not affect mitochondrial network integrity, highlighting the presence of tubular structures similar to those observed in untreated cells. A double immunocytochemistry analysis was also performed to check whether VPA treatment could induce α-syn co-localization with mitochondria, but this was not the case (Fig. 4*F*).

Considering that autophagy is activated by defects in the InsP₃-mediated Ca²⁺ release (34), autophagy levels were assayed by measuring LC3 II/LC3 I ratio in cells treated with VPA. The Western blotting and the densitometric analysis shown in Fig. 4*G* reveal that LC3 II/LC3 I ratio increased in 250 μM and 1 mM VPA-treated cells compared with untreated cells and with cells treated with 0.1–1 μM VPA. The levels of p62, another autophagy substrate, were also quantified by Western blotting and densitometric analysis (Fig. 4*G*). Interestingly, the observed increases in the autophagic process matched with a concomitant reduction in mitochondrial Ca²⁺ transients.

TAT-mediated wt α-Synuclein Delivery Affects Mitochondrial Ca²⁺ Homeostasis in Dose-dependent Manner—To exclude that the observed effects on mitochondrial Ca²⁺ were related to a general response to VPA treatment rather than to specific changes in α-syn levels and distribution, experiments were performed in HeLa cells where the α-syn intracellular concentration was increased by the exogenous addition of TAT wt α-syn fusion protein (20). As shown in Fig. 5, *A* and *B*, the Western blotting, the densitometric, and the immunocytochemistry analyses revealed a

by monitoring mtRFP fluorescence. *D,* shown is quantification of mitochondrial morphology by calculating mitochondrial circularity and form factor (see "Experimental Procedures" for details). *a.u.,* arbitrary units. A value of 1 corresponds to a perfect circle. Results are the mean ± S.E., **, $p < 0.005$, $n = 25$ cells/conditions, two independent experiments.
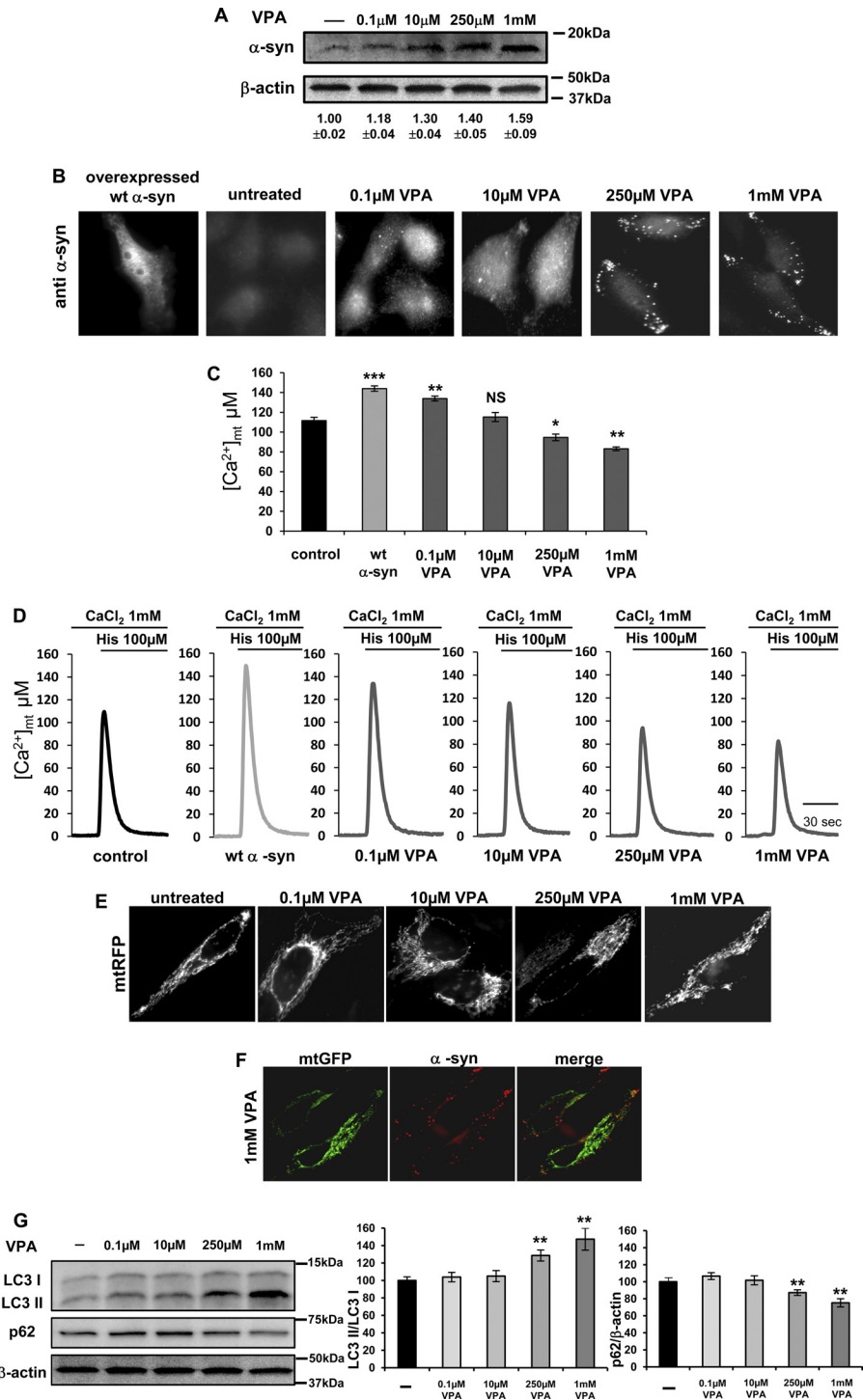
FIGURE 4. **Dose-dependent valproic acid treatment increases the endogenous content of α-synuclein, induces its redistribution to cytoplasmic foci, and affects mitochondrial Ca^{2+} transients and autophagic process.** HeLa cells were incubated with VPA in DMEM at 37 °C in CO_2 atmosphere for 6 days at the indicated doses and then transfected with mtAEQ or mtRFP or mtGFP. Western blotting (*A*) and immunocytochemistry analysis (*B*) of α-syn expression levels and distribution after VPA treatment is shown. *Numbers in panel A* refer to normalized α-syn/β-actin ratio $\pm$ S.E. in four independent Western blottings. Statistical analysis (*C*) and representative experiments (*D*) of mitochondrial Ca^{2+} measurements in HeLa cells treated with VPA are shown. Results are the mean $\pm$ S.E. ***, $p < 0.0001$; **, $p < 0.005$; *, $p < 0.01$; *NS*, not significant. Where indicated the cells were stimulated with 100 μM histamine. The traces are representative of at least five independent experiments. *E*, mitochondrial morphology in HeLa cells treated with VPA was evaluated under fluorescent microscope by observing cotransfected mtRFP. *F*, immunocytochemistry analysis with anti α-syn antibody in HeLa cells treated with 1 mM VPA and transfected with mtGFP is shown. No α-syn and mtGFP colocalization was observed in these conditions. *G*, Western blotting analysis of LC3 I, LC3 II, and p62 levels in VPA-treated cells is shown; β-actin levels were also shown. *Bars* indicate the average values obtained by densitometric analysis of five independent experiments. Results are the mean $\pm$ S.E. **, $p < 0.001$.

dose-dependent increase in the intensity of α-syn signal that paralleled α-syn redistribution from the cytoplasm to the cytosolic foci. Mitochondrial morphology was also evaluated by transfecting HeLa cells with mtGFP before TAT wt α-syn treatments; as documented in the panels of Fig. 5*B*, no alterations were observed, even at high TAT wt α-syn doses. Mitochondrial Ca^{2+} transients
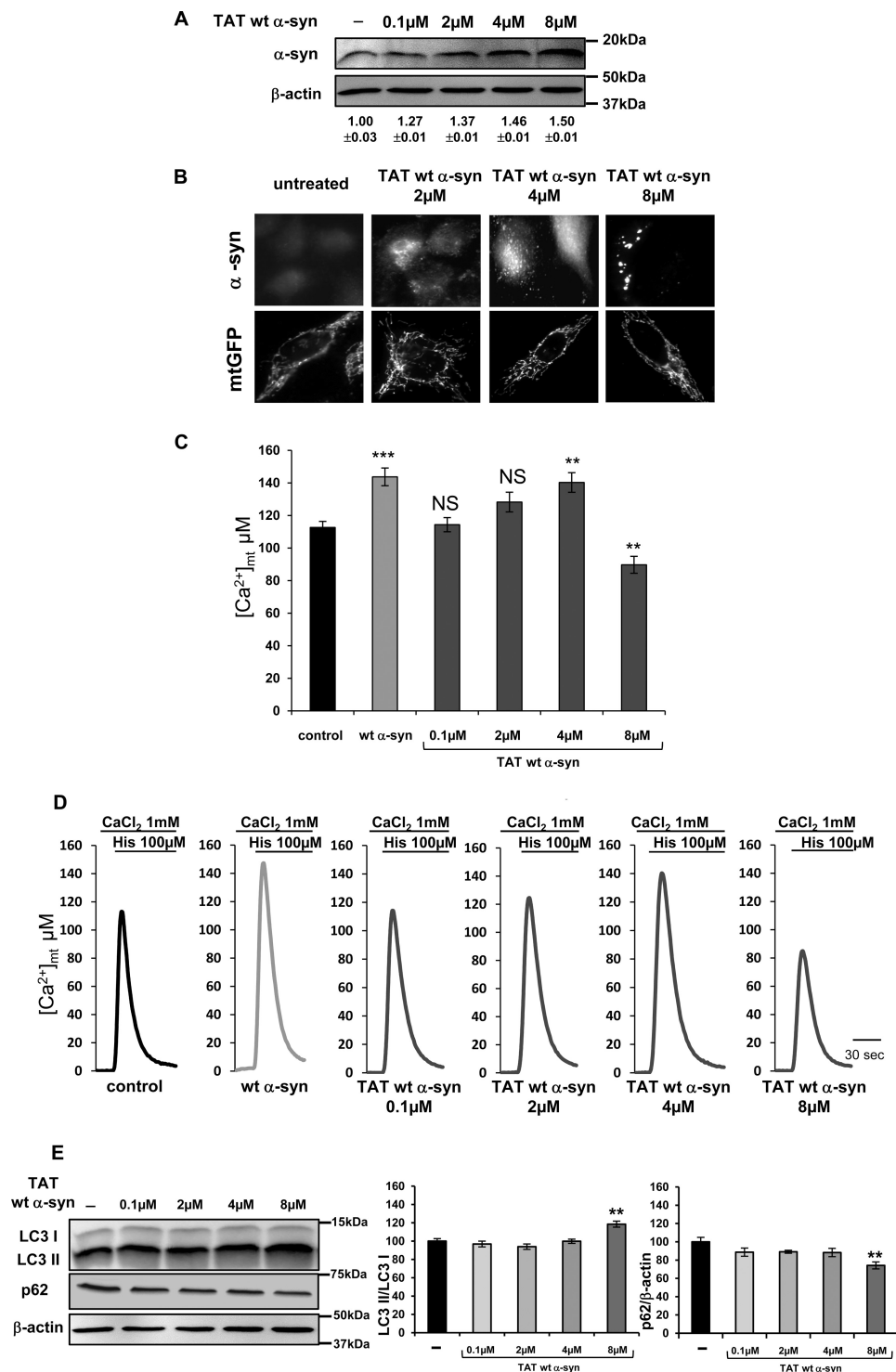
FIGURE 5. **Dose-dependent TAT-mediated wt α-synuclein delivery and effects on mitochondrial Ca²⁺ transients and autophagic process.** HeLa cells were transfected with mtGFP or mtAEQ and then incubated with the indicated doses of TAT wt α-syn. Western blotting (*A*) and immunolocalization (*B*) of TAT wt α-syn are shown. *Numbers in panel A* refer to normalized α-syn/β-actin ratio ± S.E. in three independent Western blottings. Shown is statistical analysis (*C*) and representative experiments (*D*) of mitochondrial Ca²⁺ measurements in HeLa cells treated with TAT wt α-syn. Where indicated the cells were stimulated with 100 μM histamine. *Bars* represent the mean [Ca²⁺] values upon stimulation. Results are the mean ± S.E. ***, $p < 0.0005$; **, $p < 0.005$; *NS*, not significant. The traces are representative of at least four independent experiments. *E*, shown is Western blot analysis of LC3 I, LC3 II, and p62 levels in TAT α-syn-treated cells; β-actin levels were also shown. *Bars* indicate the average values obtained by densitometric analysis of four independent experiments. Results are the mean ± S.E. **, $p < 0.001$.

were monitored by transfecting HeLa cells with mtAEQ. An initial increase of mitochondrial Ca²⁺ uptake (at 4 μM TAT wt α-syn) was followed by a decrease at 8 μM TAT wt α-syn, when α-syn is predominantly localized to cytoplasmic foci (*histograms* represent

the average peak values reached after cell stimulation and representative experiments are shown in Fig. 5, *C* and *D*; average peak values are 112.67 ± 3.72 μM, $n = 9$, in mock cells *versus* 143.75 ± 5.43 μM $n = 5$ in α-syn-overexpressing cells, $p < 0.0005$, 114.37 ±
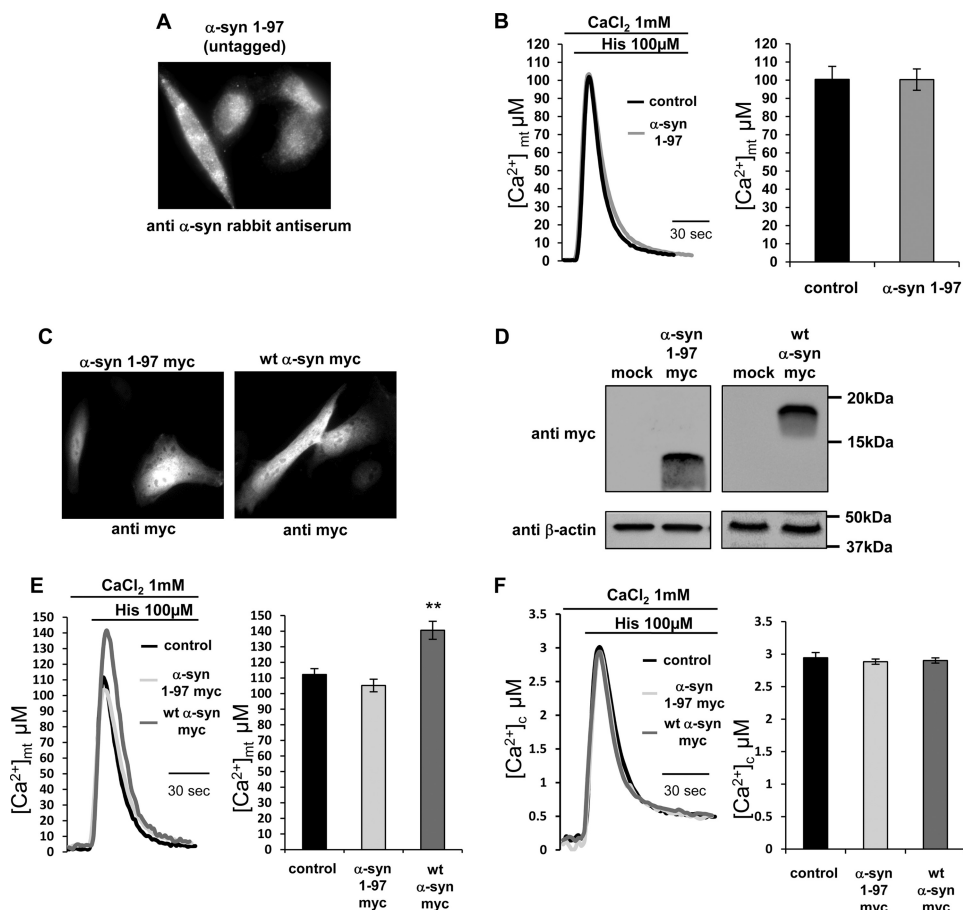
FIGURE 6. **Immunolocalization, Western blotting analysis, and Ca^{2+} measurements in HeLa cells expressing the C-terminal-truncated α-synuclein 1–97 mutant.** HeLa cells were co-transfected with mtAEQ and α-syn-(1–97) or transfected with mtAEQ and empty vector (*control*). Two different constructs expressing α-syn-(1–97) were used: an untagged version in *A* and *B* and a myc-tagged construct in *C–F*. A wt α-syn myc construct was used as comparison. Immunolocalization (*A*) and mitochondrial Ca^{2+} measurements (*B*) in HeLa cells overexpressing α-syn-(1–97) are shown. Immunolocalization (*C*), Western blotting analysis (*D*), and mitochondrial (*E*) and cytosolic (*F*) Ca^{2+} measurements in HeLa cells overexpressing wt α-syn myc or α-syn-(1–97) myc are shown. *Bars* represent mean Ca^{2+} values upon stimulation. Results are the mean ± S.E. **, $p < 0.001$. Where indicated the cells were stimulated with 100 μM histamine. The traces are representative of at least 10 independent experiments.

4.34 μM $n = 6$ in 0.1 μM TAT wt α-syn-treated cells, 128.28 ± 6.08 μM $n = 4$ in 2 μM TAT wt α-syn-treated cells, 140.30 ± 6.01 μM $n = 8$ $p < 0.005$ in 4 μM TAT wt α-syn-treated cells, and 89.73 ± 5.19 μM $n = 6$ in 8 μM TAT wt α-syn-treated cells $p < 0.005$).

To confirm the increase of the autophagic process observed in concomitance with the reduction of mitochondrial Ca^{2+} transients in VPA-treated cells, the LC3 II/LC3 I ratio was also evaluated in TAT wt α-syn-treated cells. The Western blotting and the densitometric analysis shown in Fig. 5E revealed that the LC3 II/LC3 I ratio increased in 8 μM TAT α-syn-incubated cells, and under the same conditions the level of p62 decreased accordingly to the observed reduction in mitochondrial Ca^{2+} transients.

Enhancement of Mitochondrial Ca^{2+} Uptake Depends on α-syn Acidic C-terminal Domain—Because C-terminal truncation of α-syn seems to be one of the most common post-translational modifications of α-syn in the brains of patients with PD and it was shown that substoichiometric amounts of C-terminal-truncated α-syn enhance the *in vitro* aggregation of the more abundant full-length (38), it was felt to be interesting to study the effects of the overexpression of an α-syn mutant lacking the C-terminal domain (α-syn-(1–97)). Overexpression of the deletion mutant showed a diffuse intracellular pattern of

distribution similar to the overexpressed wt α-syn as shown in Fig. 6A. In this case an anti-α-syn rabbit antiserum (kindly provided by Dr. E. Greggio, University of Padova) was used because the available α-syn monoclonal antibody previously used recognized an epitope in the C-terminal region. Unfortunately, we were not able to have it work in Western blotting. Fig. 6B shows that mitochondrial Ca^{2+} transients in α-syn-(1–97)-overexpressing cells are equivalent to those evoked in mock cells, indicating that the deletion of the C-terminal acidic domain completely abolished the ability of α-syn to enhance mitochondrial Ca^{2+} uptake (peak values: 100.4 ± 7.18 μM in mock cells $n = 10$ *versus* 100.3 ± 5.86 μM in α-syn-(1–97)-overexpressing cells $n = 10$). To better compare the effects of α-syn-(1–97) and wt α-syn, myc-tagged versions were constructed. Fig. 6, *C* and *D* document that both α-syn-(1–97) myc and wt α-syn myc were expressed and displayed a similar cytosolic distribution pattern. Fig. 6E confirms that the presence of the α-syn C-terminal tail is essential to enhance mitochondrial Ca^{2+} uptake; no differences in the mitochondrial Ca^{2+} transients generated by cell stimulation were observed between control cells and α-syn-(1–97) myc-overexpressing cells (peak values: 112.24 ± 3.71 μM in mock cells $n = 32$ *versus* 105.15 ± 4.04 μM in α-syn-(1–97)
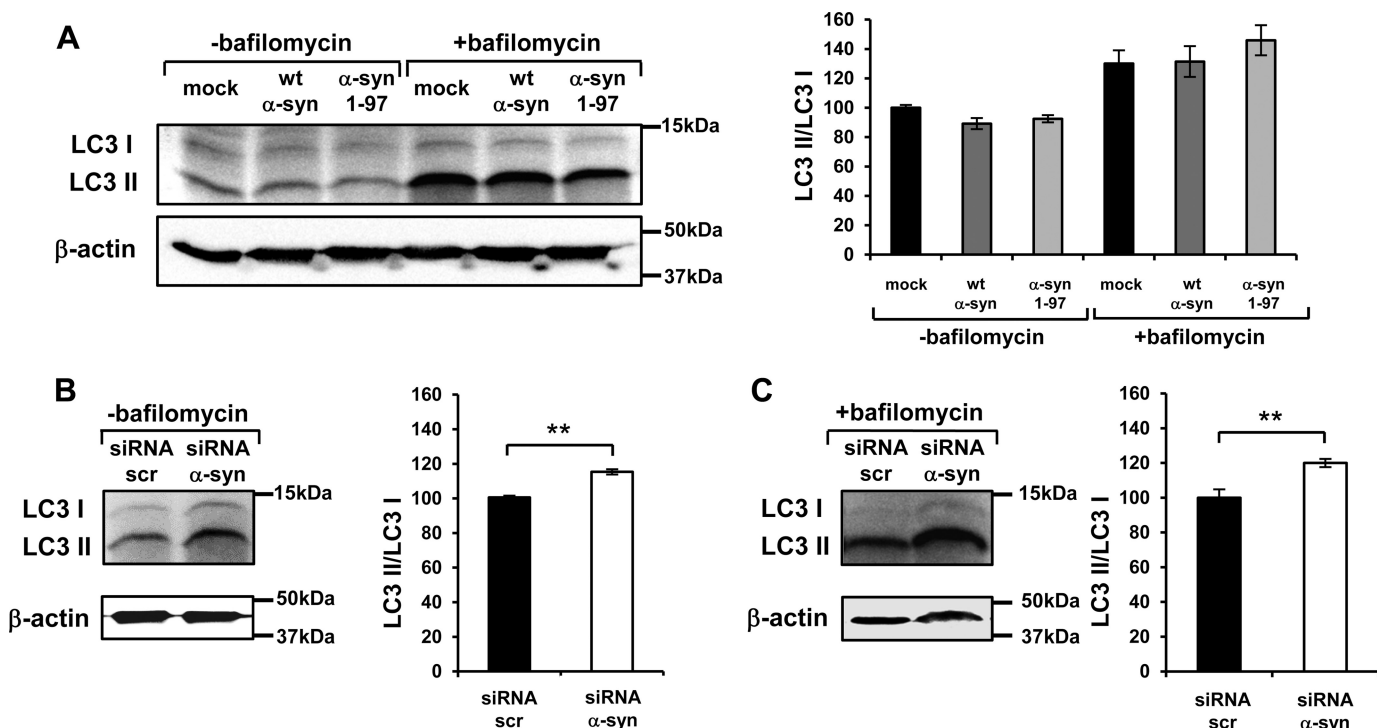
FIGURE 7. **Evaluation of autophagy process in α-syn-overexpressing cells and in siRNA α-syn-treated cells.** Western blotting analysis of LC3 I, LC3 II in wt α-syn and α-syn-(1–97)-overexpressing cells (*A*) or in α-syn siRNA-treated cells (*B* and *C*) both in the absence and in the presence of bafilomycin treatment; β-actin levels were also shown. *Bars* indicate the average values obtained by densitometric analysis of four independent experiments. Results are the mean ± S.E. **, $p < 0.001$.

myc-overexpressing cells $n = 19$), whereas the expression of wt α-syn myc induced an increase in mitochondrial Ca^{2+} transients (peak values: 140.50 ± 5.77 μM $n = 11$) similar to that monitored in wt α-syn-untagged transfected cells. The monitoring of cytosolic Ca^{2+} transients failed to reveal differences with respect to control cells in both cases (Fig. 6*F*).

The autophagic process was also evaluated. Fig. 7*A* shows that the LC3 II/LC3 I ratio in wt α-syn- and α-syn-(1–97)-overexpressing cells was similar to that of control cells (even after bafilomycin treatment), in agreement with the situation observed for concentration VPA or TAT α-syn treatments that increased or did not affect mitochondrial Ca^{2+} transients. To further strengthen the findings, autophagy was evaluated in siRNA α-syn-treated cells and in their respective control transfected with scramble siRNA (Fig. 7, *B* and *C*), and an increased LC3 II/LC3 I ratio was found in α-syn-silenced cells both in absence (Fig. 7*B*) and in presence (Fig. 7*C*) of bafilomycin treatment, as previously reported (18).

α-Synuclein Increases Functional and Physical ER-Mitochondria Interactions and Acidic C-terminal Domain Is Required to This Function—The Ca^{2+} measurements performed in permeabilized α-syn-overexpressing cells excluded the possibility that α-syn could directly affect the mitochondrial Ca^{2+} transporters activity; thus, to assess the molecular mechanisms responsible for α-syn action on mitochondrial Ca^{2+} homeostasis, the possibility that it could play a role in the formation and/or the stabilization of ER-mitochondria interactions has been investigated. First, the contribution of the ER Ca^{2+} release and that of the extracellular Ca^{2+} entry to the mitochondrial Ca^{2+} transients generation was analyzed separately. In these

experiments, HeLa cells overexpressing either wt or α-syn-(1–97) were perfused in KRB containing 100 μM EGTA buffer and stimulated with 100 μM histamine; under these conditions a peak transient was generated reflecting the mitochondrial response to ER Ca^{2+} mobilization. Then the perfusion medium was switched to KRB supplemented with 2 mM $CaCl_2$ (in the continuous presence of histamine), thus causing Ca^{2+} entry from the extracellular milieu that was primarily sensed by mitochondria located beneath the plasma membrane. The mitochondrial Ca^{2+} peak in response to ER Ca^{2+} mobilization (first peak) was significantly higher in cells overexpressing wt α-syn as compared with control cells; that in response to Ca^{2+} influx (second peak) was instead reduced (Fig. 8, *A* and *B*). As expected, in α-syn-(1–97) mutant-overexpressing cells, no effect was observed on mitochondrial Ca^{2+} transients, being the first and second peak equivalent to those of control cells (Fig. 8, *A* and *B*). The reduction of the second peak in α-syn-overexpressing cells is probably due to the effect of α-syn on Ca^{2+} influx induced by store depletion as previously documented (see "Discussion" and Ref. 39).

Second, to directly test the possible involvement of α-syn in regulating ER-mitochondria contact sites, we performed live-cell confocal microscopy three-dimensional reconstructions of ER and mitochondria. HeLa cells were co-transfected with the mtRFP- and ER-targeted-GFP (erGFP) together with either wt α-syn or α-syn-(1–97) mutant, and ER-mitochondria co-localization was assessed. The single plane level analysis revealed a significant increase in ER-mitochondria contact sites in wt α-syn-overexpressing cells compared with mock cells, but not in α-syn-(1–97) mutant-overexpressing cells, as documented
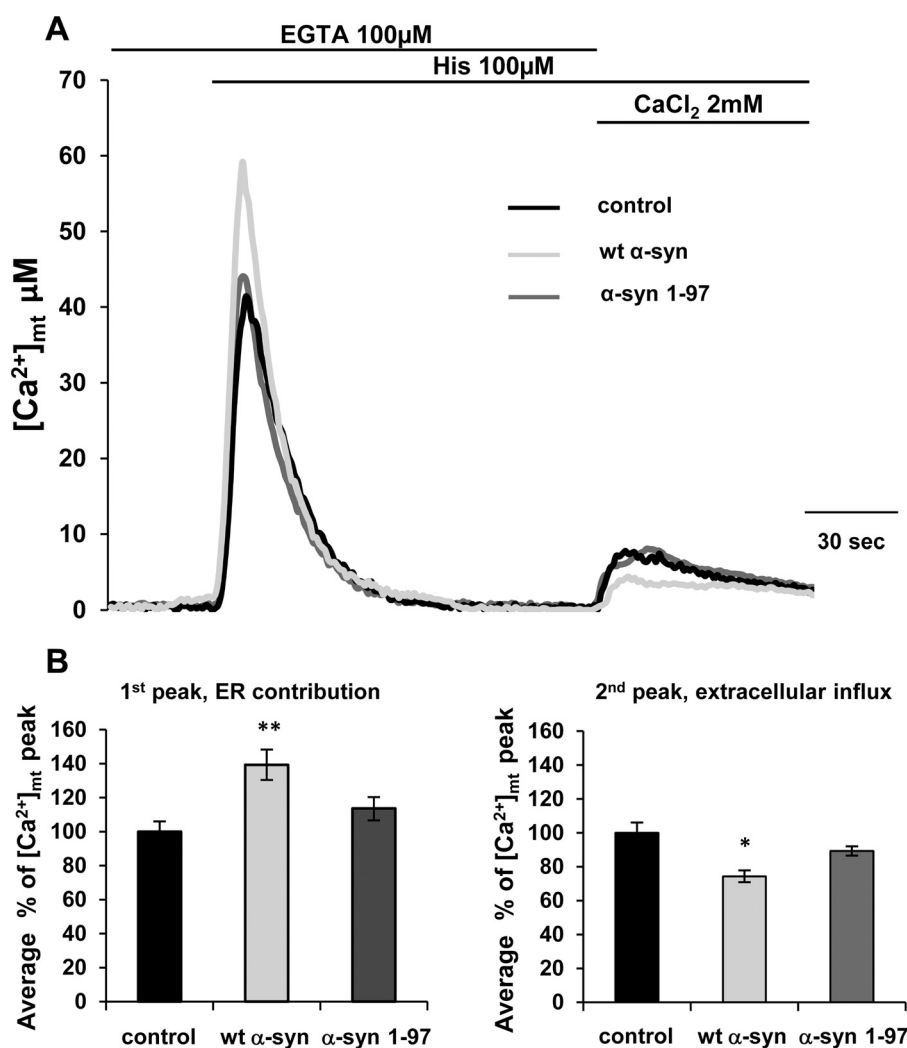
FIGURE 8. **Evaluation of the contribution of ER Ca²⁺ mobilization and of Ca²⁺ influx from the extracellular ambient on mitochondrial Ca²⁺ transients in wt and α-synuclein 1–97-overexpressing cells.** HeLa cells were co-transfected with mtAEQ and α-syn constructs or transfected with mtAEQ only (control). To discriminate the contributions to $[Ca^{2+}]_m$ transients, InsP₃-induced Ca²⁺ release from intracellular stores was separated from the concomitant Ca²⁺ influx across the plasma membrane. *A*, HeLa cells were perfused in KRB/EGTA 100 μM buffer and stimulated with histamine to release Ca²⁺ from the intracellular stores (*first peak*). Then, the perfusion medium was switched to KRB/Ca²⁺ 2 mM (in the continuous presence of histamine) to stimulate Ca²⁺ entry from the extracellular ambient (*second peak*). The traces are representative of at least 13 independent experiments. *B*, bars represent normalized mean [Ca²⁺] values upon stimulation, and results are the mean ± S.E. **, $p < 0.001$; *, $p < 0.01$.

in the merging images of Fig. 9*A*. A more detailed quantification was carried out by acquiring confocal *z* axis stacks, applying volume rendering on the three-dimensional reconstructions and calculating the Manders' colocalization coefficient (31). Also with this analysis an enhancement in the ER/mitochondria co-localization was observed in α-syn-overexpressing cells with respect to mock-treated cells (mock cells, $100 \pm 1.34\%$, $n = 71$ cells, and wt α-syn $109.23 \pm 1.04\%$, $n = 21$ cells, $p < 0.0001$), but not in α-syn-(1–97) mutant-expressing cells ($103.4 \pm 1.04\%$, $n = 37$ cells), as documented in Fig. 9, *B* and *C*.

DISCUSSION

A possible direct involvement of α-syn in Ca²⁺ homeostasis in living cells has been described by few reports, but the results were conflicting. An increase in membrane conductance and in cytosolic basal Ca²⁺ levels as well as augmented cytosolic Ca²⁺ transients were reported in A53T-expressing cells with respect to wt α-syn-expressing cells (40). Hettiarachchi *et al.* (39) in

2009 have instead shown that voltage-gated Ca²⁺ entry was similarly enhanced in neuronal cells expressing wt and mutant α-syn and that the Ca²⁺ influx pathways triggered by store depletion were significantly suppressed in wt α-syn-, A53T-, and S129D-expressing cells. Basal cytosolic Ca²⁺ levels and ER and mitochondria Ca²⁺ content were instead unaffected. A couple of reports described that overexpression of wt α-syn as well as that of A53T mutant enhanced the mitochondria ability to accumulate Ca²⁺ (16, 41), suggesting that α-syn-overexpressing cells could be more prone to mitochondrial Ca²⁺ overload, but the possibility that these increases could be physiological rather than pathological has not been considered. Mitochondria are essential for cell survival because they are involved in energy metabolism, cell signaling, and regulation in intracellular Ca²⁺ homeostasis: their integrity is a key element for cell wellness. At the functional level, our study demonstrates that the α-syn is essential to maintain mitochondrial integrity and metabolism and that its depletion significantly reduces
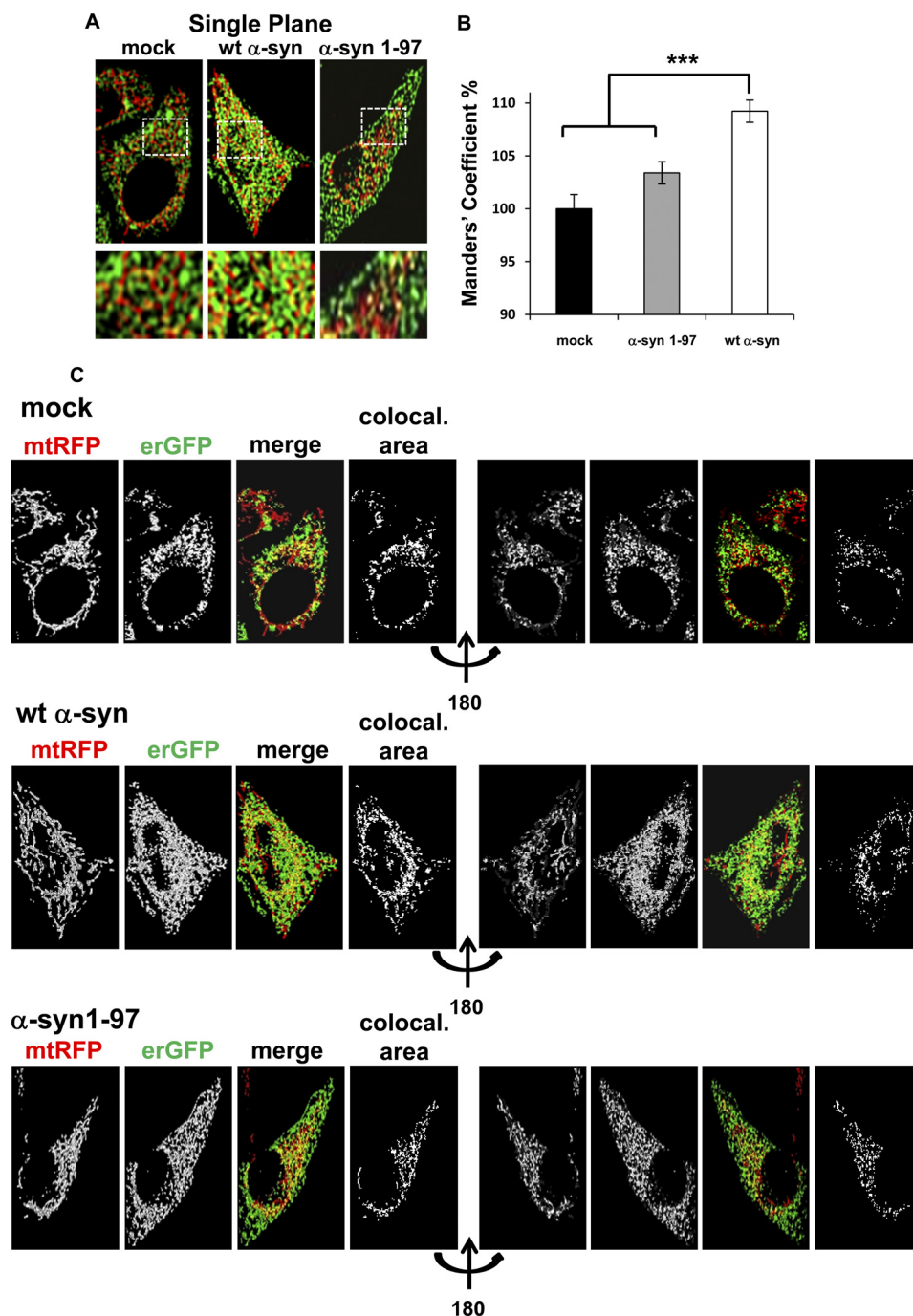
FIGURE 9. **ER-mitochondria interactions in HeLa cells overexpressing wt α-synuclein and truncated α-synuclein 1–97.** *A*, shown are single plane confocal images showing ER (*green*, erGFP) and mitochondria (*red*, mtRFP) co-localization in mock or wt -syn or wt α-syn-(1–97)-transfected cells. *Insets* at higher magnification are also shown. *B*, *bars* represent normalized Manders' coefficient values calculated from z-axis confocal stacks. At least 21 cells were analyzed for each conditions (results are the mean ± S.E. ***, $p < 0.0001$). *C*, shown is three-dimensional reconstruction of mitochondria and ER in HeLa cells coexpressing mtRFP and an erGFP together with the void vector (*mock*), wt α-syn, or α-syn-(1–97) as indicated in each panel. Cells were excited separately at 488 or 543 nm, and the single images were recorded. The merging of the two images is shown for each condition. *Yellow* indicates colocalization of the two organelles. A better view of the area of colocalization is provided by the *panels on the right*. Confocal stacks were acquired every 0.2 μm along the z axis (for a total of 40 images) with a 63× objective.

agonist-stimulated Ca^{2+} entry in mitochondrial matrix. We also found that wt α-syn overexpression induces an increase in the mitochondrial Ca^{2+} transients evoked by cell stimulation and that the entity of the transients is compatible with physiological levels of mitochondrial Ca^{2+} concentration. Intriguingly, by controlling these levels, α-syn also modulates the autophagic process; defects in ER-mitochondria Ca^{2+} transfer

result in an activated autophagy, as previously documented (34).

The mechanism of these effects was investigated, and the results obtained in permeabilized cells excluded that α-syn could act in modulating the activity of mitochondrial Ca^{2+} transporters. Rather, evidence was obtained that α-syn plays a role in regulating the mitochondria/ER relationship. It is well

known that mitochondria, despite the low affinity of the uniporter, can efficiently take up Ca^{2+} because sense high Ca^{2+} concentrations microdomains generated at the mouth of Ca^{2+} channels. In particular, in HeLa cells (but also in other cells type) mitochondria have been demonstrated to be juxtaposed to the $InsP_3$ receptors, the main Ca^{2+} release channels of the ER, which also participate in the formation of contact sites (42). The ER-mitochondria contact sites were directly monitored and quantified by analyzing three-dimensional reconstructions of confocal images acquired from living cells co-transfected with erGFP and mtRFP and α-syn. Intriguingly, wt α-syn overexpression resulted in an increased tethering of the two organelles, whereas α-syn-(1–97) had no effects. The finding is particularly interesting because the intimate connection between ER and mitochondria has been reported to be at the basis of a bidirectional communication regulating a number of physiological processes ranging from mitochondrial energy production and lipid metabolism to Ca^{2+} signaling and cell death (43–45). Interestingly, the α-syn acidic C-terminal domain seems to be responsible for the observed phenotype, as the overexpression of α-syn-(1–97) mutant (in which the last 43 C-terminal residues were removed) failed to affect the mitochondrial Ca^{2+} transients and the formation of ER-mitochondria contact sites. Whether the presence of phosphorylation sites (*i.e.* Tyr-125, Tyr-133, and Tyr-136 or Ser 129) is necessary to this function is presently unknown. The C terminus has no structural elements, it has been shown to be necessary but not sufficient for a chaperone function (46), and it is thought that interactions between the C terminus and the central portion of the α-syn molecule may prevent or minimize aggregation/fibrillation (47).

In addition to the overexpression protocol, two alternative experimental procedures were used to increase the intracellular levels of α-syn: the VPA treatment and TAT-mediated delivery. Both of them confirmed the results obtained in α-syn-overexpressing cells and added new information on the possible mechanism of α-syn action. At high doses of VPA or TAT α-syn fusion protein, the increase in the α-syn expression levels correlated with a change in its intracellular distribution; the α-syn fluorescence is confined to punctuated cytoplasmic foci, and no diffuse cytosolic fluorescence signal was observed. When mitochondrial Ca^{2+} measurements were performed in these cells, a drastic reduction in mitochondrial Ca^{2+} transients was observed despite that the mitochondrial morphology was apparently unaltered. These data together with those obtained in α-syn siRNA experiments suggest that mitochondrial Ca^{2+} impairment possibly started before mitochondrial structure derangements, and it is related to α-syn sequestration out of the cytosol, thus proposing loss of function mechanism as responsible for mitochondrial dysfunction reported in dopaminergic cells of α-syn-related PD models. Interestingly, α-syn loss of function in addition to the effects on mitochondrial Ca^{2+} fluxes also resulted in increased autophagy, as documented both in α-syn siRNA and VPA or TAT α-syn-treated cells.

Our data also indicated that α-syn is required to maintain the mitochondrial network integrity as its down-regulation (but not its overexpression) clearly revealed a pattern of fragmented mitochondria. These results partially matched with recent data

in the literature; some reports described no mitochondrial fragmentation upon α-syn overexpression (41), but others, even if through different mechanisms, have reported induced mitochondrial fragmentation (17, 19). These apparent discrepancies may be ascribed to the different expression level in cell models, the dose-dependent pathogenic role for the wt protein when overexpressed being well established (7). Even if we have not done accurate measurements of mitochondria volume and length, we can confidentially state that in our cell system, α-syn overexpression did not induce mitochondria fragmentation not only by the evaluation of mitochondrial morphology at fluorescence and confocal microscope but also because we found that that α-syn overexpression enhanced mitochondrial Ca^{2+} transients, the opposite to what it has been found in cells overexpressing the pro-fission protein Drp1 (48).

Altogether the data presented here indicate that α-syn is required for maintaining mitochondrial Ca^{2+} homeostasis and network integrity and for potentiating the ER-mitochondria connection, its C terminus acidic domain being essential to these functions. Some hypothesis can be done on the possible mechanisms; one intriguing possibility is that α-syn directly mediated the ER-mitochondria interaction by acting as a "bridge." This mechanism is strongly supported by the finding that the molecular chaperone grp75 has been found to interact with α-syn (49, 50), and interestingly enough, grp75 has been demonstrated to couple $InsP_3$ receptors with VDAC, the voltage-dependent anion channel of the outer mitochondrial membrane, and in this way to regulate the mitochondria Ca^{2+} uptake machinery (42).

As far as PD is concerned, several reports describe the fundamental contribution of mitochondria and ER to the cellular fate as well as a privileged communication between the two organelles as a key element for cell functions (7, 51, 52).

In summary, we have demonstrated that α-syn, by favoring Ca^{2+} transfer from the ER to mitochondria, sustains organelle function and morphological integrity. When the protein is defective, Ca^{2+} uptake is reduced, and mitochondria undergo massive fragmentation. Interestingly, it has been recently reported that *in vivo* RNAi-mediated α-syn silencing induces nigrostriatal degeneration and that the level of neurodegeneration correlates with the grade of down-regulation of α-syn protein and mRNA (53). When, however, protein is expressed at high levels, it is redistributed to cytosolic foci (7), and this also leads to the loss of its effect on mitochondrial signaling and to the increase of autophagic process. Overall, the data point to Ca^{2+}-mediated signaling in mitochondria as an important site where α-syn can modulate cell bioenergetics and survival.

REFERENCES

1. Hirsch, E. C., Hunot, S., Faucheux, B., Agid, Y., Mizuno, Y., Mochizuki, H., Tatton, W. G., Tatton, N., and Olanow, W. C. (1999) Dopaminergic neurons degenerate by apoptosis in Parkinson disease. *Mov. Disord.* **14,** 383–385

2. Spillantini, M. G., Schmidt, M. L., Lee, V. M., Trojanowski, J. Q., Jakes, R., and Goedert, M. (1997) α-Synuclein in Lewy bodies. *Nature* **388,** 839–840

3. Thomas, B., and Beal, M. F. (2007) Parkinson disease. *Hum. Mol. Genet.* **16,** R183–R194

4. Shavali, S., Brown-Borg, H. M., Ebadi, M., and Porter, J. (2008) Mitochondrial localization of α-synuclein protein in α-synuclein-overexpressing cells. *Neurosci. Lett.* **439,** 125–128

5. Cole, N. B., Dieuliis, D., Leo, P., Mitchell, D. C., and Nussbaum, R. L. (2008) Mitochondrial translocation of α-synuclein is promoted by intracellular acidification. *Exp. Cell Res.* **314,** 2076–2089

6. Devi, L., Raghavendran, V., Prabhu, B. M., Avadhani, N. G., and Anandatheerthavarada, H. K. (2008) Mitochondrial import and accumulation of α-synuclein impair complex I in human dopaminergic neuronal cultures and Parkinson disease brain. *J. Biol. Chem.* **283,** 9089–9100

7. Auluck, P. K., Caraveo, G., and Lindquist, S. (2010) α-Synuclein. Membrane interactions and toxicity in Parkinson disease. *Annu. Rev. Cell Dev. Biol.* **26,** 211–233

8. Burré, J., Sharma, M., Tsetsenis, T., Buchman, V., Etherton, M. R., and Südhof, T. C. (2010) α-Synuclein promotes SNARE-complex assembly *in vivo* and *in vitro*. *Science* **329,** 1663–1667

9. Nemani, V. M., Lu, W., Berge, V., Nakamura, K., Onoa, B., Lee, M. K., Chaudhry, F. A., Nicoll, R. A., and Edwards, R. H. (2010) Increased expression of α-synuclein reduces neurotransmitter release by inhibiting synaptic vesicle reclustering after endocytosis. *Neuron* **65,** 66–79

10. Chinta, S. J., Mallajosyula, J. K., Rane, A., and Andersen, J. K. (2010) Mitochondrial α-synuclein accumulation impairs complex I function in dopaminergic neurons and results in increased mitophagy *in vivo*. *Neurosci. Lett.* **486,** 235–239

11. Loeb, V., Yakunin, E., Saada, A., and Sharon, R. (2010) The transgenic overexpression of α-synuclein and not its related pathology associates with complex I inhibition. *J. Biol. Chem.* **285,** 7334–7343

12. Dauer, W., Kholodilov, N., Vila, M., Trillat, A. C., Goodchild, R., Larsen, K. E., Staal, R., Tieu, K., Schmitz, Y., Yuan, C. A., Rocha, M., Jackson-Lewis, V., Hersch, S., Sulzer, D., Przedborski, S., Burke, R., and Hen, R. (2002) Resistance of α -synuclein null mice to the parkinsonian neurotoxin MPTP. *Proc. Natl. Acad. Sci. U.S.A.* **99,** 14524–14529

13. Klivenyi, P., Siwek, D., Gardian, G., Yang, L., Starkov, A., Cleren, C., Ferrante, R. J., Kowall, N. W., Abeliovich, A., and Beal, M. F. (2006) Mice lacking α-synuclein are resistant to mitochondrial toxins. *Neurobiol. Dis.* **21,** 541–548

14. Martin, L. J., Pan, Y., Price, A. C., Sterling, W., Copeland, N. G., Jenkins, N. A., Price, D. L., and Lee, M. K. (2006) Parkinson disease α-synuclein transgenic mice develop neuronal mitochondrial degeneration and cell death. *J. Neurosci.* **26,** 41–50

15. Hsu, L. J., Sagara, Y., Arroyo, A., Rockenstein, E., Sisk, A., Mallory, M., Wong, J., Takenouchi, T., Hashimoto, M., and Masliah, E. (2000) α-Synuclein promotes mitochondrial deficit and oxidative stress. *Am. J. Pathol.* **157,** 401–410

16. Parihar, M. S., Parihar, A., Fujita, M., Hashimoto, M., and Ghafourifar, P. (2008) Mitochondrial association of α-synuclein causes oxidative stress. *Cell. Mol. Life Sci.* **65,** 1272–1284

17. Kamp, F., Exner, N., Lutz, A. K., Wender, N., Hegermann, J., Brunner, B., Nuscher, B., Bartels, T., Giese, A., Beyer, K., Eimer, S., Winklhofer, K. F., and Haass, C. (2010) Inhibition of mitochondrial fusion by α-synuclein is rescued by PINK1, Parkin, and DJ-1. *EMBO J.* **29,** 3571–3589

18. Winslow, A. R., Chen, C. W., Corrochano, S., Acevedo-Arozena, A., Gordon, D. E., Peden, A. A., Lichtenberg, M., Menzies, F. M., Ravikumar, B., Imarisio, S., Brown, S., O'Kane, C. J., and Rubinsztein, D. C. (2010) α-Synuclein impairs macroautophagy. Implications for Parkinson disease. *J. Cell Biol.* **190,** 1023–1037

19. Nakamura, K., Nemani, V. M., Azarbal, F., Skibinski, G., Levy, J. M., Egami, K., Munishkina, L., Zhang, J., Gardner, B., Wakabayashi, J., Sesaki, H., Cheng, Y., Finkbeiner, S., Nussbaum, R. L., Masliah, E., and Edwards, R. H. (2011) Direct membrane association drives mitochondrial fission by the Parkinson disease-associated protein α-synuclein. *J. Biol. Chem.* **286,** 20710–20726

20. Albani, D., Peverelli, E., Rametta, R., Batelli, S., Veschini, L., Negro, A., and

21. Forloni, G. (2004) Protective effect of TAT-delivered α-synuclein. Relevance of the C-terminal domain and involvement of HSP70. *FASEB J.* **18,** 1713–1715

21. Brini, M. (2008) Calcium-sensitive photoproteins. *Methods* **46,** 160–166

22. Rizzuto, R., Brini, M., Bastianutto, C., Marsault, R., and Pozzan, T. (1995) Photoprotein-mediated measurement of calcium ion concentration in mitochondria of living cells. *Methods Enzymol.* **260,** 417–428

23. Rizzuto, R., Brini, M., Murgia, M., and Pozzan, T. (1993) Microdomains with high Ca^{2+} close to IP3-sensitive channels that are sensed by neighboring mitochondria. *Science* **262,** 744–747

24. Rapizzi, E., Pinton, P., Szabadkai, G., Wieckowski, M. R., Vandecasteele, G., Baird, G., Tuft, R. A., Fogarty, K. E., and Rizzuto, R. (2002) Recombinant expression of the voltage-dependent anion channel enhances the transfer of Ca^{2+} microdomains to mitochondria. *J. Cell Biol.* **159,** 613–624

25. Brini, M., Marsault, R., Bastianutto, C., Alvarez, J., Pozzan, T., and Rizzuto, R. (1995) Transfected aequorin in the measurement of cytosolic Ca^{2+} concentration ($[Ca^{2+}]c$). A critical evaluation. *J. Biol. Chem.* **270,** 9896–9903

26. Barrero, M. J., Montero, M., and Alvarez, J. (1997) Dynamics of $[Ca^{2+}]$ in the endoplasmic reticulum and cytoplasm of intact HeLa cells. A comparative study. *J. Biol. Chem.* **272,** 27694–27699

27. Duchen, M. R., Surin, A., and Jacobson, J. (2003) Imaging mitochondrial function in intact cells. *Methods Enzymol.* **361,** 353–389

28. Nerem, R. M., Levesque, M. J., and Cornhill, J. F. (1981) Vascular endothelial morphology as an indicator of the pattern of blood flow. *J. Biomech. Eng.* **103,** 172–176

29. Dagda, R. K., Cherra, S. J., 3rd, Kulich, S. M., Tandon, A., Park, D., and Chu, C. T. (2009) Loss of PINK1 function promotes mitophagy through effects on oxidative stress and mitochondrial fission. *J. Biol. Chem.* **284,** 13843–13855

30. de Brito, O. M., and Scorrano, L. (2008) Mitofusin 2 tethers endoplasmic reticulum to mitochondria. *Nature* **456,** 605–610

31. Manders, E. M., Verbeek, F. J., and Aten, J. A. (1993) Measurement of colocalization of objects in dual-color confocal images. *J. Microsc.* **169,** 375–382

32. Rizzuto, R., Pinton, P., Carrington, W., Fay, F. S., Fogarty, K. E., Lifshitz, L. M., Tuft, R. A., and Pozzan, T. (1998) Close contacts with the endoplasmic reticulum as determinants of mitochondrial Ca^{2+} responses. *Science* **280,** 1763–1766

33. Nakamura, K., Nemani, V. M., Wallender, E. K., Kaehlcke, K., Ott, M., and Edwards, R. H. (2008) Optical reporters for the conformation of α-synuclein reveal a specific interaction with mitochondria. *J. Neurosci.* **28,** 12305–12317

34. Cárdenas, C., Miller, R. A., Smith, I., Bui, T., Molgó, J., Müller, M., Vais, H., Cheung, K. H., Yang, J., Parker, I., Thompson, C. B., Birnbaum, M. J., Hallows, K. R., and Foskett, J. K. (2010) Essential regulation of cell bioenergetics by constitutive InsP3 receptor Ca^{2+} transfer to mitochondria. *Cell* **142,** 270–283

35. Koopman, W. J., Verkaart, S., Visch, H. J., van der Westhuizen, F. H., Murphy, M. P., van den Heuvel, L. W., Smeitink, J. A., and Willems, P. H. (2005) Inhibition of complex I of the electron transport chain causes O[bardot,2]-mediated mitochondrial outgrowth. *Am. J. Physiol. Cell Physiol.* **288,** C1440–C1450

36. Leng, Y., and Chuang, D. M. (2006) Endogenous α-synuclein is induced by valproic acid through histone deacetylase inhibition and participates in neuroprotection against glutamate-induced excitotoxicity. *J. Neurosci.* **26,** 7502–7512

37. Gitler, A. D., Bevis, B. J., Shorter, J., Strathearn, K. E., Hamamichi, S., Su, L. J., Caldwell, K. A., Caldwell, G. A., Rochet, J. C., McCaffery, J. M., Barlowe, C., and Lindquist, S. (2008) The Parkinson disease protein α-synuclein disrupts cellular Rab homeostasis. *Proc. Natl. Acad. Sci. U.S.A.* **105,** 145–150

38. Li, W., West, N., Colla, E., Pletnikova, O., Troncoso, J. C., Marsh, L., Dawson, T. M., Jäkälä, P., Hartmann, T., Price, D. L., and Lee, M. K. (2005) Aggregation promoting C-terminal truncation of α-synuclein is a normal cellular process and is enhanced by the familial Parkinson disease-linked mutations. *Proc. Natl. Acad. Sci. U.S.A.* **102,** 2162–2167

39. Hettiarachchi, N. T., Parker, A., Dallas, M. L., Pennington, K., Hung, C. C., Pearson, H. A., Boyle, J. P., Robinson, P., and Peers, C. (2009) α-Synuclein modulation of Ca²⁺ signaling in human neuroblastoma (SH-SY5Y) cells. *J. Neurochem.* **111,** 1192–1201

40. Furukawa, K., Matsuzaki-Kobayashi, M., Hasegawa, T., Kikuchi, A., Sugeno, N., Itoyama, Y., Wang, Y., Yao, P. J., Bushlin, I., and Takeda, A. (2006) Plasma membrane ion permeability induced by mutant α-synuclein contributes to the degeneration of neural cells. *J. Neurochem.* **97,** 1071–1077

41. Marongiu, R., Spencer, B., Crews, L., Adame, A., Patrick, C., Trejo, M., Dallapiccola, B., Valente, E. M., and Masliah, E. (2009) Mutant Pink1 induces mitochondrial dysfunction in a neuronal cell model of Parkinson disease by disturbing calcium flux. *J. Neurochem.* **108,** 1561–1574

42. Szabadkai, G., Bianchi, K., Várnai, P., De Stefani, D., Wieckowski, M. R., Cavagna, D., Nagy, A. I., Balla, T., and Rizzuto, R. (2006) Chaperone-mediated coupling of endoplasmic reticulum and mitochondrial Ca²⁺ channels. *J. Cell Biol.* **175,** 901–911

43. Csordás, G., and Hajnóczky, G. (2009) SR/ER-mitochondrial local communication. Calcium and ROS. *Biochim. Biophys. Acta* **1787,** 1352–1362

44. Rizzuto, R., Marchi, S., Bonora, M., Aguiari, P., Bononi, A., De Stefani, D., Giorgi, C., Leo, S., Rimessi, A., Siviero, R., Zecchini, E., and Pinton, P. (2009) Ca²⁺ transfer from the ER to mitochondria. When, how. and why. *Biochim. Biophys. Acta* **1787,** 1342–1351

45. de Brito, O. M., and Scorrano, L. (2010) An intimate liaison: spatial organization of the endoplasmic reticulum-mitochondria relationship. *EMBO J.* **29,** 2715–2723

46. Park, S. M., Jung, H. Y., Kim, T. D., Park, J. H., Yang, C. H., and Kim, J. (2002) Distinct roles of the N-terminal binding domain and the C-terminal-solubilizing domain of α-synuclein, a molecular chaperone. *J. Biol. Chem.* **277,** 28512–28520

47. Ulrih, N. P., Barry, C. H., and Fink, A. L. (2008) Impact of Tyr to Ala mutations on α-synuclein fibrillation and structural properties. *Biochim. Biophys. Acta* **1782,** 581–585

48. Szabadkai, G., Simoni, A. M., Chami, M., Wieckowski, M. R., Youle, R. J., and Rizzuto, R. (2004) Drp-1-dependent division of the mitochondrial network blocks intraorganellar Ca²⁺ waves and protects against Ca²⁺-mediated apoptosis. *Mol. Cell* **16,** 59–68

49. Jin, J., Li, G. J., Davis, J., Zhu, D., Wang, Y., Pan, C., and Zhang, J. (2007) Identification of novel proteins associated with both α-synuclein and DJ-1. *Mol. Cell. Proteomics* **6,** 845–859

50. Burbulla, L. F., Schelling, C., Kato, H., Rapaport, D., Woitalla, D., Schiessling, C., Schulte, C., Sharma, M., Illig, T., Bauer, P., Jung, S., Nordheim, A., Schöls, L., Riess, O., and Krüger, R. (2010) Dissecting the role of the mitochondrial chaperone mortalin in Parkinson disease. Functional impact of disease-related variants on mitochondrial homeostasis. *Hum. Mol. Genet.* **19,** 4437–4452

51. Arduíno, D. M., Esteves, A. R., Cardoso, S. M., and Oliveira, C. R. (2009) Endoplasmic reticulum and mitochondria interplay mediates apoptotic cell death. Relevance to Parkinson disease. *Neurochem. Int.* **55,** 341–348

52. Calì, T., Ottolini, D., and Brini, M. (2011) Mitochondria, calcium, and endoplasmic reticulum stress in Parkinson disease. *Biofactors* **37,** 228–240

53. Gorbatyuk, O. S., Li, S., Nash, K., Gorbatyuk, M., Lewin, A. S., Sullivan, L. F., Mandel, R. J., Chen, W., Meyers, C., Manfredsson, F. P., and Muzyczka, N. (2010) *In vivo* RNAi-mediated α-synuclein silencing induces nigrostriatal degeneration. *Mol. Ther.* **18,** 1450–1457